

Supplementary material

Computational investigation of promising Si-Cu anode material

Alexander Y. Galashev^{a,b,*} and Ksenia A. Ivanichkina^a

^a*Institute of High-Temperature Electrochemistry, Ural Branch, Russian Academy of Sciences,
Sofia Kovalevskaya Str. 22, Yekaterinburg 620990, Russia*

^b*Ural Federal University named after the first President of Russia B.N. Yeltsin
Mira Str., 19, Yekaterinburg 620002, Russia*

Some details of the computer experiment

Table 1

Parameters of Morse potential describing various interactions

Interaction*	D_0 (meV)	α (nm ⁻¹)	r_m
Si ⁽¹⁾ -Si ⁽²⁾	227.40	44.992	0.154
Li-Li	420.76	7.899	0.300
Li-Si	309.30	36.739	0.116
Li-Cu	379.84	10.743	0.293
Cu-Si	279.24	14.489	0.359

* The upper indices at Si denote the belonging to the layer of atoms 1 or 2

The initial distance between ions introduced was not less than 1 nm. Lithium ions with an integer electric charge of +1e experienced reciprocal Coulomb repulsion in addition to the Morse interaction characteristic of electrically neutral Li atoms. At a distance of 1 nm, the interaction energy of two point elementary charges is about 1.44 eV. To move an elementary point charge at a distance of 1 nm along the field line of force, it is necessary to perform a work of 3.69 eV. This is 1.7 times more than the binding energy between lithium and silicene (2.2 eV / atom). The Li atom has a very low diffusion barrier in silicon (~ 0.6 eV) [1]. The interaction of silicene with the substrate and with Li atoms adsorbed and the presence of vacancy defects in silicene can change the silicone buckle height Δh and the Si-Si bond length \bar{L} . We observed changes in buckle height and bond lengths in the ranges of $0.06 \leq \Delta h \leq 0.12$ nm and $0.231 \leq \bar{L} \leq 0.243$ nm, respectively. Thus, we obtained good agreement with the values of the average Si-Si bond length for Si₄₀₀

* Corresponding author.

E-mail address: galashev@ihete.uran.ru (A.Y. Galashev).

nanoparticles in the vitrified (0.242 nm) and amorphous state (0.236 nm) [2]. The average Si-Li bond length obtained was 0.265 nm, which is in good agreement with the data of [3]. The adsorption energy values determined for lithium by us on silicene were from 2.27 to 2.52 eV / Li (depending on the location of the Li atom).

To determine the effect of the silicene channel on the ion transfer of the Li⁺ ion, we performed two separate calculations in the presence of the same electric field (10³ V / m). In the first case, the ion moved along a flat silicon channel, having a gap of 2 nm, at $T = 300$ K, and in the second, in vacuum at $T = 0$ K. In the channel, the ion passed a distance of 5.1 nm for 10 ps reflecting from the walls. In vacuum, the ion traveled a distance of 115 times less during a time 10 times greater than in the first experiment. Consequently, when an ion moves through a flat channel, the electric field only plays the role of a certain guiding force. In general, the dynamics of the ion motion (including the trajectory) are determined by the thermal motion of surrounding atoms and the collisions of the ion with them.

The perfect silicene sheet contained 300 atoms. We also performed calculations for channels whose walls are not formed by an ideal silicene. In this case, 9 vacancy defects were formed in each sheet of silicene. Four types of defects were considered: mono-, bi-, tri-, and hexavacancies. Nine identical defects were placed approximately evenly with a shift of 0.1–0.2 nm in each (x and y) direction for different silicene sheets. A channel with hexavacancies on a copper substrate quickly collapsed when filled with lithium. The results of this series of calculations are not presented in this article. Silicene sheet containing mono-, bi-, and trivacancies was formed from 291, 282, 273 Si atoms, respectively. The stacking of Bernal (ABAB ...) was exactly the same as for the graphene sheets in graphite, which was carried out while creating flat, perfect and defective silicene channels [4]. The copper substrate contained 1536 atoms, which were located in the four (111) planes of the corresponding crystal. The equations of motion were solved by the Runge-Kutta method of order 4.

When using the LAMMPS program [5], the system should not lose particles during the calculation, i.e. none of the atoms must go beyond the rectangular container. Such a container was created using the imposed force field. At the initial moment of time, the distance from any Si or Cu atom to the nearest container wall was not less than 0.5 nm, and the distance from Si atoms of the upper sheet of silicene to the upper wall of the container was 1.15 nm. Li⁺ ions (or Li atoms) interacted with the wall only when they approached it at a distance of $r < R_{\text{cutoff}} = 0.25$ nm. This interaction occurred in accordance with the Lennard-Jones potential (12-6) with parameters $\sigma = 0.1$ nm, $\varepsilon = 1$ eV. These parameters do not correspond to any real material. They are chosen empirically in order to obtain an adequate model for studying the processes of intercalation /

deintercalation. When the distance to the wall was less than 0.1 nm, the repulsive force acting from the wall returned the atom (ion) back to the system.

The lithium was intercalated into the silicon channel by means of the simultaneous emission of two Li^+ ions from randomly selected points on a line having constant coordinates $x = 0.198$ nm, $z = 0.375$ nm. Moreover, these points were separated by a distance not less than 1 nm and each of them was no closer than 0.2 nm from the centers of the extreme silicon atoms belonging to the “zigzag” border of the sheets. Thus, the line of the initial points was slightly shifted into the channel, passing through the middle of the channel gap. A constant electric field of 10^3 V / m, acting on ions during their lifetime (10 ps), served as a guiding and pushing force. During this time, the ions often had time to find a favorable location on the surface of the silicene. If this did not happen, they turned into atoms and continued to find such places along with other atoms. The search for fixing points in the channel as a whole here seems to be a stochastic process. Therefore, there is no need to make the lifetime of an ion a stochastic variable.

During the lifetime (10 ps), the Li^+ ion could not leave the channel, since been unable to overcome the barrier created by the attracting interaction of other atoms. When the ion turned into an atom, it lost an electrical charge. Loss of charge, i.e. turning into an atom led to the insensitivity of this particle to the action of an electric field. However, the newly born atom continued to interact with all other atoms in the model as before. A pairwise launch of Li^+ ions into the channel was performed every 10 ps. The procedure for launching ions stopped as soon as the ions (or ion) were not able to enter the channel or left it during their lifetime. In the case of a channel formed by sheets of perfect silicon, the limiting number of Li atoms filling the channel was 48. This value almost 19% exceeded the value of the lithium limit filling of the corresponding channel on an Ag (111) substrate. Five more attempts were made to supplement the channel with Li^+ ions, but all of them were unsuccessful. All the described actions were also performed when filling the silicene channels, the walls of which had vacancy-type defects. After the completion of intercalation, particles with an electric charge, i.e. ions absented in the system.

Deintercalation began with the fact that a pair of atoms, which were the last of the remaining ones, when the channel was filled with lithium, acquired an electric charge. The formed ions Li^+ under the influence of the electric field moved through the channel and eventually left it. The ions left the channel always alone, without being accompanied by other atoms. We conducted a separate study, in which random atoms constituted an ion pair. This study showed that the order in which atoms acquire an electric charge does not affect the overall picture of deintercalation. As before, the ions left the channel without taking other Li atoms with them.

Additional information about the results

Table 2.

Changes in the channel volume (relative to the initial state before filling the channel with lithium) at its maximum filling with lithium and after complete lithium deintercalation in the silicene channels on a copper substrate

Process direction	Cu(111) substrate				
	Type of vacancy defects				
	perfect	monovacancies	bivacancies	trivacancies	hexavacancies
intercalation	+4.2%	-13.4%	-19.1%	-14.6%	-13.63%
deintercalation	+8.82%	-1.96%	+2.4%	+2.3%	silicene destruction

Table 3.

Change of the distance between the Cu(111) substrate and the silicene channel (relative to the initial state of the system until the channel is filled with lithium) at the maximum saturation of the channel with lithium and after its complete clearing

Process direction	Cu(111) substrate					
	Type of vacancy defects					
	Initial Cu-Si distance, nm	perfect	mono-	bi-	tri-	hexa-
intercalation	0.27	+15.3%	+29.6%	+26.6%	+25.2%	36.1%
deintercalation		+32.2%	+25.9%	+22.9%	+23.1%	silicene destruction

Abbreviations

MD	Molecular dynamics
VPs	Voronoi polyhedra
SPs	Simplified polyhedral

During intercalation, the longest period of U_{Li} decline is observed in a system with the perfect silicene, and the shortest period is when there are bi-vacancies in silicene. In the presence of trivacancies in silicene at the initial period of deintercalation, the energy U_{Li} retains the values acquired during intercalation. After remaining about 20 Li atoms in the channel, there was a fast increase in the value of U_{Li} under deintercalation. The fast growth of U_{Li} is due to increase in the deceleration energy of ions (per atom) with a decrease in the number of atoms in the channel.

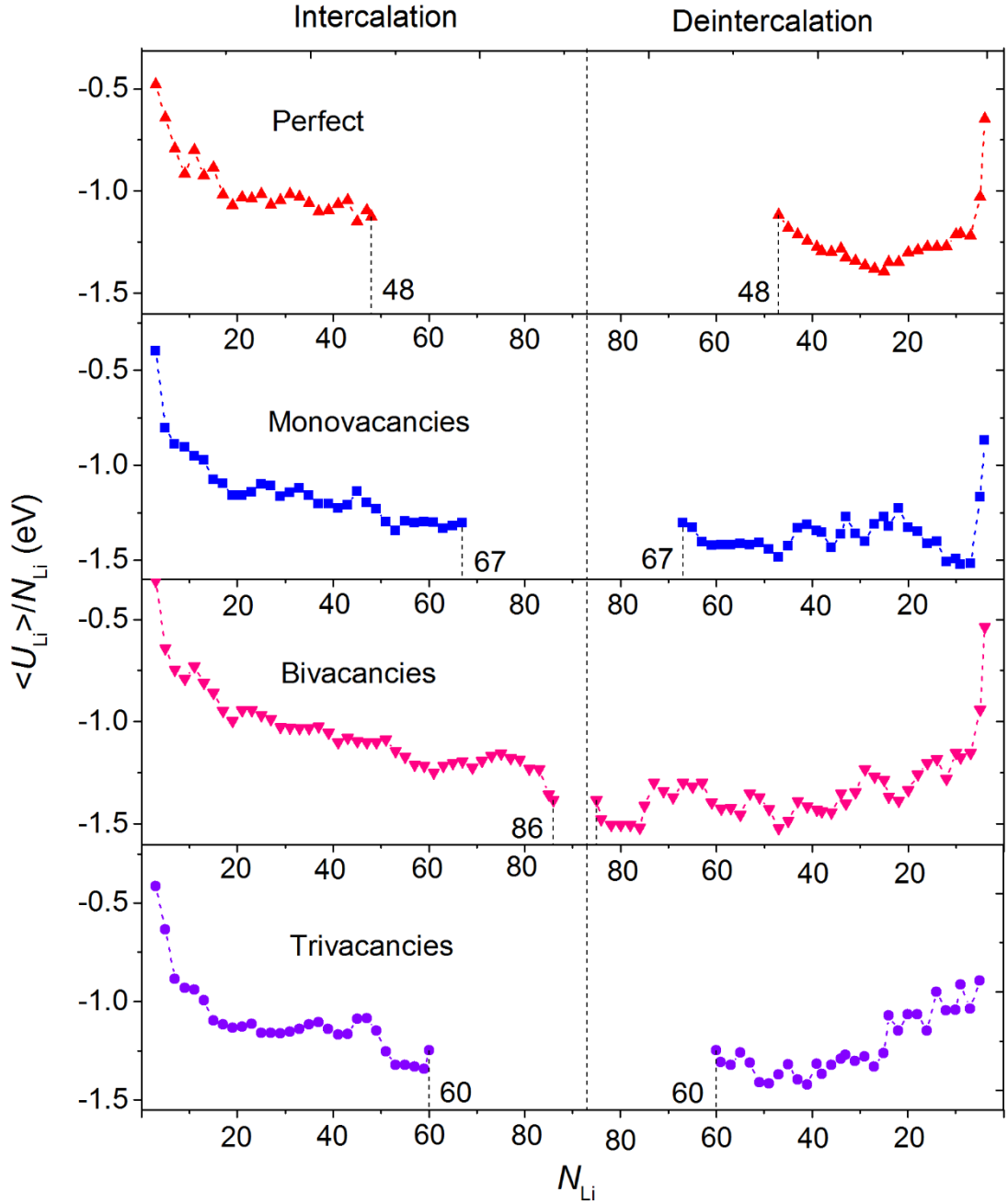


Fig. A1. The total energy of lithium atoms in the process of intercalation (left) and deintercalation (right) in silicene channels with the perfect silicene and silicene having mono-, bi-, and trivacancies.

During intercalation, when the number of Li atoms in the channel becomes larger than 20, the relief of the channel walls begins to exert a strong influence on the mobility of the Li atoms. In this connection, the value of D can both decrease (in the presence of mono-vacancies) and increase (in the case of bi-vacancies). The value of D also behaves quite unpredictably in the case of deintercalation. This value is subject to narrow (for the perfect silicene) and wide (for silicene with mono-vacancies) bursts during deintercalation. The coefficient D in this process may decrease. In the presence of bivacancies, this happens with the help of fluctuation changes, and when trivacancies.

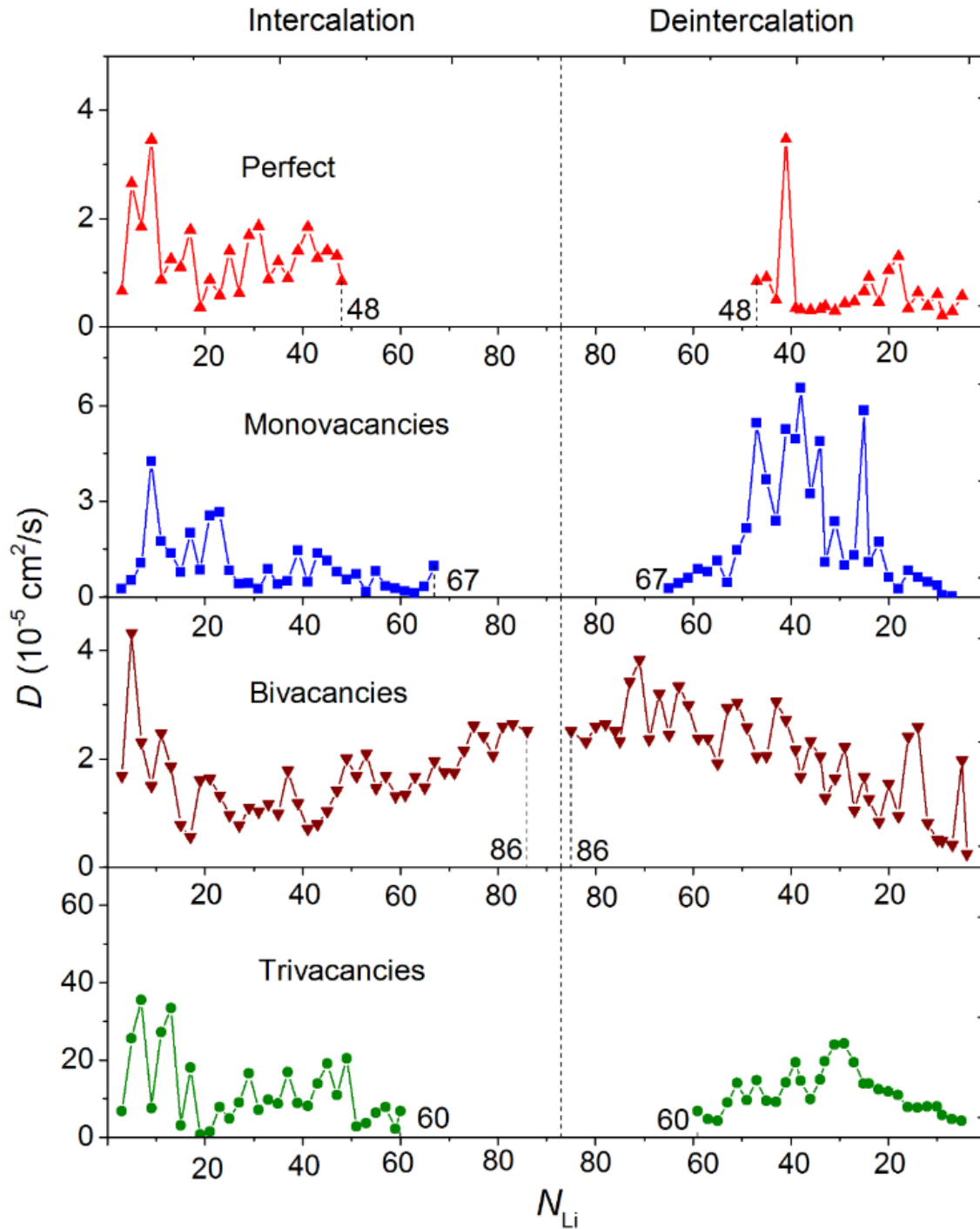


Fig. A2. The coefficient of self-diffusion of lithium atoms in the process of intercalation (left) and deintercalation (right) in silicene channels with perfect silicene and silicene having mono-, bi-, and trivacancies.

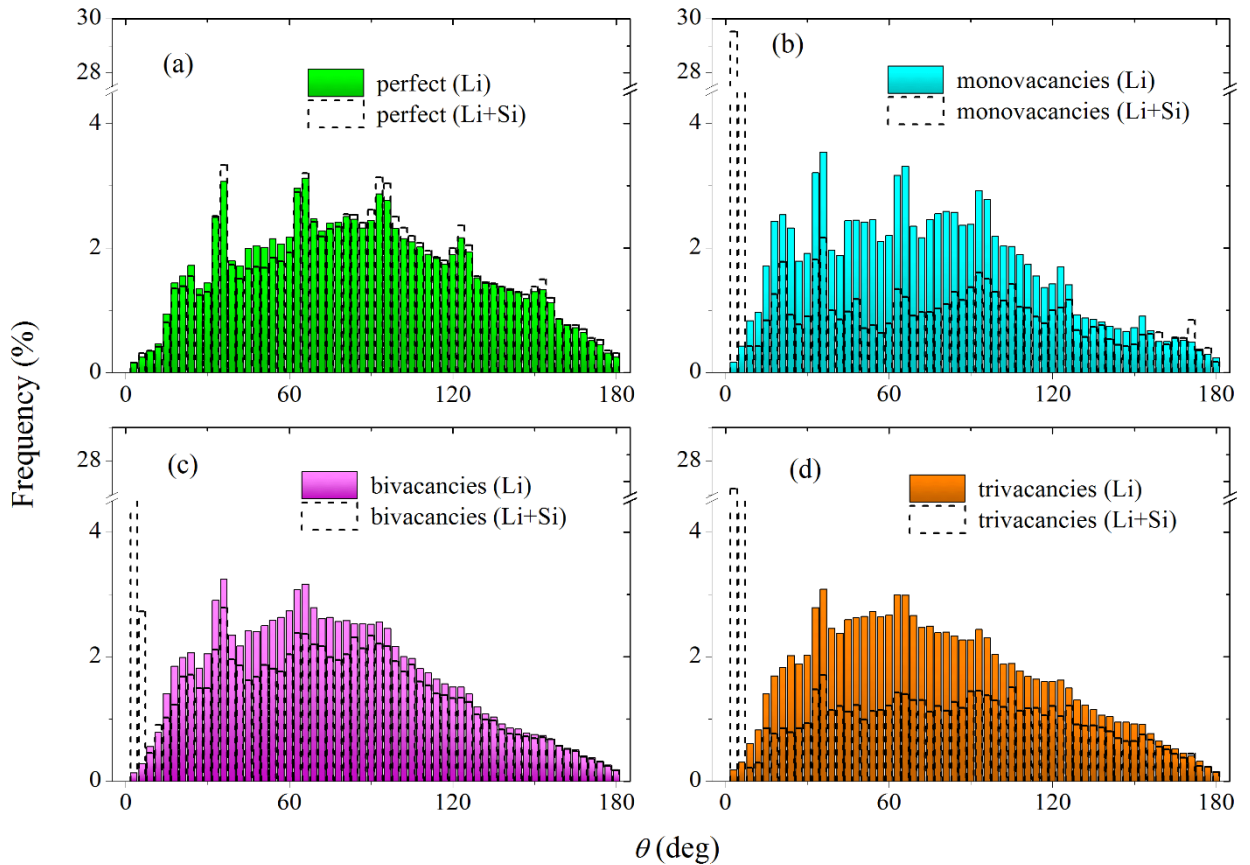


Fig. A3. The angular distribution of the nearest neighbors for lithium atoms in the period of intercalation. Voronoi polyhedral (VPs) are built for lithium atoms after the complete filling of a silicon channel, which is located: (a) - (d) on an Cu(111) substrate. Solid (colored) histograms present the case when neighbors are represented only by Li atoms, dotted histograms give an idea of the local packing of atoms when neighbors are selected from both Li atoms and Si atoms. The types of defects in silicene and considered neighbors (in parentheses) are indicated in the captions in the margins of figures (a) - (d).

Exclusion of small geometric elements, i.e. the transition to simplified polyhedral (SP) allows one to find obvious structural differences in the packing of Li atoms in the silicene channels on different metal substrates.

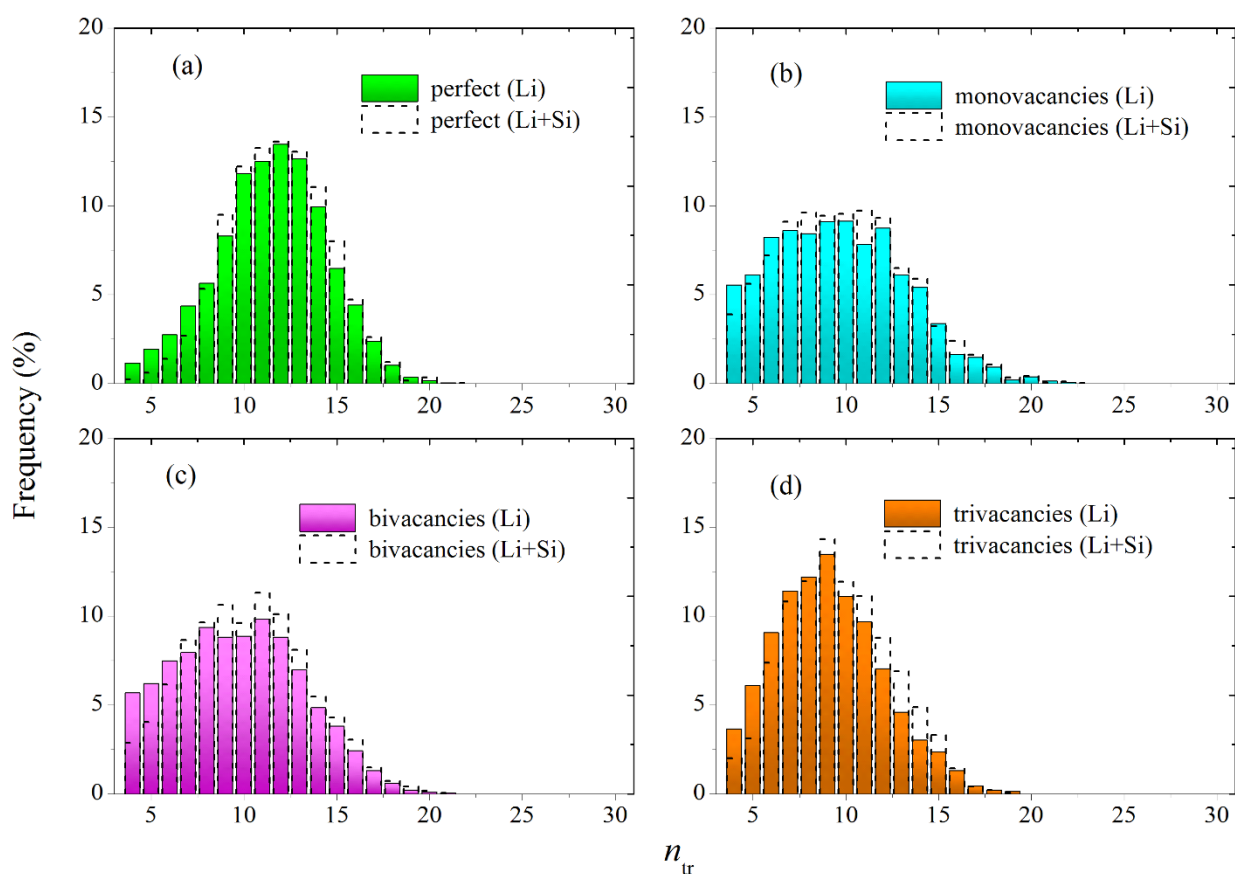


Fig. A4. The distribution of truncated polyhedra (simplified, SP) with respect to the number of faces (n_{tr}) in the period of deintercalation, when 30 Li atoms are left in the channel: (a) - (d) on a Cu(111) substrate. Solid (colored) histograms present the case when neighbors are represented only by Li atoms, dotted histograms give an idea of the local packing of atoms when neighbors are selected from both Li atoms and Si atoms. The types of defects in silicene and considered neighbors (in parentheses) are indicated in the captions in the margins of figures (a) - (d).

DFT method

Our calculations were performed using the SIESTA [1, 2] package, which implements density functional theory (DFT) with the pseudopotential approximation and a basis set of linear combination of atomic orbital [3, 4]. Bulk silicon and copper DOS spectra calculation used a $2 \times 2 \times 2$ Monkhorst-Pack k-meshes in conjunction with a 64 (Si) and 108 (Cu)-atom supercell and periodic boundary conditions (PBC). To study the band structure of a silicene monolayer sheet on a copper substrate, a 2×2 supercell was constructed, consisting of 8 Si atoms. The buckle height in silicene was 0.064 nm. The metal substrate was defined by 16 metal atoms located in 2 planes of 8 atoms each. Initially, the planes were separated from the lower silicene sublattice at distances of 0.270 nm and 0.478 nm. In the $0x$, $0y$ directions, ordinary PBC were used. The translation vector in the $0z$ direction was chosen to be 1.5 nm. To improve the computational speed, we performed geometric optimization using the Purdue–Burke–Erzerhof generalized gradient procedure (PBE) [5]. The tolerances for optimizing the geometry at full energy were within 5.0×10^{-6} eV/atom. The maximum Hellmann–Feynman force was within $0.01 \text{ eV} \cdot \text{\AA}^{-1}$. The geometry of all structures was completely optimized.

Adhesion energy calculation

Adhesion energy is a measure of the connection between dissimilar surfaces or an atom (molecule) brought into contact with a surface. In the case of the deposition of lithium or copper atoms on silicene, the adhesion energy is defined as [11]

$$E_{\text{ad}} = [n_{\text{Me}} E_{\text{Me}} + n_{\text{Si}} E_{\text{Si}} - E_{\text{Me+Si}}] / N, \quad (1)$$

where E_{Me} , E_{Si} denote the single-atom energy of atoms Me and Si, respectively, n_{Me} , n_{Si} are the number of Me and Si atoms contained in the unit cell, respectively; $E_{\text{Me+Si}}$ denotes the total energy of single-layer silicene and Me(111) substrate, N is the number of total atoms contained in the unit cell. It is possible that both the adsorbed atom (Li) and the substrate (Cu) are metal, then in the above notation, Si should be replaced by Cu.

The adhesion energy was calculated for atoms located above the center of the hexagonal silicon ring or above the well between the three atoms of the Cu (111) substrate. Both the quantum-mechanical MD calculation (*ab initio*) and the classical MD calculation were performed in order to select the Morse parameters of the potential describing the cross-interaction. As a result, the following agreement was reached between the calculated values of adhesion energy: Li-silicene - 2.08 (-2.01) eV [11], Li-Cu (111) -2.57 (-2.48) eV, Cu-silicene -2.95 (-2.87) eV. The lengths of

the Li–Si (0.279 nm), Li–Cu (0.247 nm), and Cu– Si (0.243 nm) bonds obtained in *ab initio* calculations agree within 10% with the corresponding data of the classical MD calculation. All MD calculations were performed at $T = 300$ K. In *ab initio* calculations, the size of the simulated system was reduced to 78 Si atoms in a silicene sheet and to 98 atoms in a single Cu sheet. In quantum MD calculations, lower E_{ad} values are obtained, which may be associated not only with the inaccuracy of the description of cross-interaction with the Morse potential, but also with different sizes of simulated systems and a significantly shorter (1 ps) observation time of the system when *ab initio* molecular dynamics are used compared to classic MD calculations (100 ps).

References

1. A. E. Galashev, Yu. P. Zaikov and R. G. Vladykin, Effect of electric field on lithium ion in silicene channel. Computer experiment. Rus. J. Electrochem. 2016, **52**, 966–974.
2. A. E. Galashev, I. A. Izmodenov, A. N. Novruzov and O. A. Novruzova, Computer study of physical properties of silicon nanostructures. Semiconductors 2017, **41**, 190–196.
3. T. H. Osborn and A. A. Farajian, Stability of lithiated silicene from first principles. J. Phys. Chem. C 2012, **116**, 22916–22920.
4. A. E. Galashev and O. R. Rakhmanova, Numerical simulation of heating an aluminum film on two-layer graphene. High Temp. 2014, **52**, 374–380.
5. S. Plimpton, Fast parallel algorithms for short-range molecular dynamics. J. Comp. Phys. 1995, **117**, 1–19.
6. P. Ordejon, E. Artacho, J. M. Soler, Self-consistent order-N density-functional calculations for very large systems. Phys. Rev. B 1996, **53**, 10441–10444.
7. D. Sanchez-Portal, P. Ordejon, E. Artacho, J. M. Soler, Density functional method for very large systems with LCAO basis sets. Int. J. Quantum Chem. 1997, **65**, 453–461.
8. P. Hohenberg, W. Kohn, Inhomogeneous electron gas. Phys. Rev. B 1964, **136**, 864–871.
9. W. Kohn, L. J. Sham, Self-consistent equations including exchange and correlation effects. Phys. Rev. A 1965, **140**, 1133–1138.
10. J. P. Perdew, K. Burke, M. Ernzerhof, Generalized gradient approximation made simple. Phys. Rev. Lett. 1996, **77**, 3865–3868.
11. A. Y. Galashev, A. S. Vorob'ev, Physical properties of silicene electrodes for Li-, Na-, Mg-, and K-ion batteries. J. Solid State Electrochem. 2018, **22**, 3383–3391.